Biochimica et Biophysica Acta, 352 (1974) 97–116

BBA 76637

RED BLOOD CELL CALCIUM AND MAGNESIUM: EFFECTS UPON SODIUM AND POTASSIUM TRANSPORT AND CELLULAR MORPHOLOGY*

MICHAEL J. DUNN**
with the technical assistance of RUTH GRANT

Department of Medicine, Division of Nephrology, University of Vermont, College of Medicine, Burlington, Vt. 05401 (U.S.A.)

(Received December 27th, 1973)

SUMMARY

Previous studies have established that intracellular divalent cations, especially Ca^{2+}, have important effects on erythrocyte membrane function. We set out to increase intracellular Ca^{2+}, and to increase or decrease intracellular Mg^{2+} in fresh, ATP-rich, human erythrocytes. Since these cells, unlike those of many previous studies, were not ATP depleted, conclusions could be drawn concerning the effects of divalent cations upon energy-dependent transport processes.

Intracellular Ca^{2+} (Ca_i^{2+}) had more dramatic influence on the cells than did Mg^{2+}. When Ca_i^{2+} was increased progressively from normal (0.015 mM) to 2 mM there was a reciprocal fall in ouabain-inhibited Na^+ efflux. Na^+ influx, a measure of Na^+ permeability, increased. The net effect of these changes was to increase intracellular Na^+. Intracellular K^+ decreased more rapidly than Na^+ increased. These alterations of transport were accompanied by echinocytic and spherocytic deterioration of cellular shape and a 20% decrement of cellular size as assessed by scanning electron microscopy. When these high-Ca_i^{2+} cells were incubated in substrate-rich medium for 24 h, Ca^{2+} was eliminated from the cells. Pari passu, the membrane transport of Na^+ and K^+ returned towards normal with substantial reductions of intracellular Na^+ and increments of K^+. Improvement of the morphologic alterations was also observed. Increasing intracellular Mg^{2+} stimulated active Na^+ efflux whereas lowering intracellular Mg^{2+} had no apparent influence on Na^+ efflux. No evidence of active Mg^{2+} efflux could be found.

We conclude that intracellular Ca^{2+}, in human erythrocytes, is a critical determinant of cellular size, shape and transport of cations. The influence of Ca^{2+} is easily noted without energy depletion. The observed changes are partially reversible.

INTRODUCTION

Intracellular divalent cations (Ca_i^{2+} and Mg_i^{2+}) in erythrocytes affect many membrane functions including rate of hemolysis, cation transport, cell size and shape,

* This work was published in abstract form, in 1973, Clin. Res. 21, 552.

** Dr Dunn is a Scholar in Academic Medicine, John and Mary Markle Foundation.

Abbreviation: PCMBS, *p*-chloromercuribenzene sulfonate.

viscosity and deformability [1–9]. Schatzman and others [10–13] have confirmed recently that Ca^{2+} is excluded from the interior of the erythrocyte by virtue of an efficient Ca^{2+}-efflux pump. This is an ATP-dependent, Ca^{2+}–ATPase linked, ouabain-insensitive efflux mechanism capable of Ca^{2+} transport against an electrochemical gradient [10–13]. The maintenance of a low intracellular Ca^{2+} level is imperative since the detrimental effects of Ca^{2+} on the erythrocyte membrane, are restricted to the interaction of Ca_i^{2+} and the internal surface of the membrane [14]. Extracellular Ca^{2+} (Ca_o^{2+}) has no effect [14, 15]. No similar Mg^{2+} -transport system has been identified and unlike Ca_i^{2+}, Mg_i^{2+} is greater than Mg_o^{2+} [16]. Previous investigations of these inter-relationships have utilized erythrocytes ghosts, and ATP depleted intact erythrocytes. The present study utilized fresh human erythrocytes with alterations of Ca_i^{2+} or Mg_i^{2+} which were induced through reversible manipulation of membrane cation permeability using trinitrocresol or *p*-chloromercuribenzene sulfonate. This allowed an assessment of the effects of Ca_i^{2+} and Mg_i^{2+} on fresh, ATP-replete, intact human erythrocytes. Parameters measured included net Na^+, K^+, Ca^{2+} and Mg^{2+} fluxes, tracer Na^+ fluxes, and erythrocyte size and morphology under scanning electron microscopy. Our results confirm the belief that the level of Ca_i^{2+} is of critical importance to the cell with regard to all parameters measured. Changes of Mg_i^{2+} produced fewer alterations.

METHODS

Increasing intracellular calcium (Ca_i^{2+})

1.0 mM trinitrocresol (Eastman Kodak, Rochester, N.Y.) was used to enhance calcium entry into the cell. Previously trinitrocresol had been shown to increase the permeability of erythrocytes to monovalent cations and to decrease permeability of erythrocytes to anions [17]. The present studies confirm that erythrocytes also have enhanced permeability to divalent cations. Fresh human erythrocytes were obtained in heparin, washed with saline, separated from the buffy coat and refrigerated (0–4 °C) at an 8–10% hematocrit in the following solution: $CaCl_2$, either 10 mM, 5 mM or none; NaCl, 10 mM; KCl, 147 mM; $MgCl_2$, 2 mM and trinitrocresol, 1.0 mM. After 16 h refrigeration the trinitrocresol-treated cells were removed by centrifugation and washed six times with a cold solution similar to the refrigeration medium, except for the omission of trinitrocresol and a $CaCl_2$ concentration of 1.0 mM for those cells in which an elevated Ca_i^{2+} was desired. Washing was completed with three final washes with 295 mosM NaCl. These cells were then used for net and tracer flux measurements, scanning electron microscopy and determination of Ca_i^{2+}, Na_i^+ and K_i^+.

Alterations of intracellular magnesium (Mg_i^{2+})

Parachloromercuribenzene sulfonate (PCMBS) (Sigma Chemicals, St. Louis, Mo.) was used to enhance the permeability of the erythrocytes to Mg^{2+} [18]. Preliminary experiments showed PCMBS to be at least tenfold more effective than trinitrocresol for this purpose. We also found that ATP depletion enhanced Mg_i^{2+} losses and therefore the cells for the low Mg_i^{2+} studies were depleted of ATP for 4–24 h in sterile glucose-free solutions prior to manipulation of Mg^{2+}. Erythrocytes were refrigerated for 36–48 h for low Mg_i^{2+} and 16–24 h for high Mg_i^{2+} in the following solutions:

PCMBS, 0.1 mM; KCl, 147 mM; NaCl, 14 mM; Na_2HPO_4–NaH_2PO_4 (pH 7.4), 295 mosM; 6 mM Na^+; $MgCl_2$, 2 mM for controls, zero for low Mg_i^{2+} and 40 mM for high Mg_i^{2+}. After the refrigeration the erythrocytes were separated by centrifugation and incubated for 3 h at 37 °C in solutions similar to the PCMBS medium but omitting PCMBS and adding the sulfhydryl reagent, dithiothreitol (5 mM), to remove the sulfhydryl inhibitory effect of PCMBS [19], 0.1 g/100 ml albumin, and 10 mM glucose, 3 mM adenine, and 10 mM inosine to restore ATP [20]. After 3 h these erythrocytes were removed, washed three times with 295 mosM NaCl and used for net and tracer flux determinations and measurement of Mg_i^{2+}. Erythrocyte ATP, measured using phosphoglycerate kinase and assaying NADH disappearance [21], was normal or high after the reconstitution procedure.

Measurement of Ca_i^{2+} and Mg_i^{2+}

The erythrocytes were washed three times (for Mg_i^{2+}) or five times (for Ca_i^{2+}) with 295 mosM NaCl. A known volume of cells was lysed in 7.5 mM $LaCl_3$ and Mg^{2+} determined by atomic absorption spectrophotometry. For measurement of Ca_i^{2+} by atomic absorption spectroscopy, the washed erythrocytes were lysed and the protein extracted with 5.0% trichloracetic acid. This extract was subsequently diluted with 7.5 mM $LaCl_3$. All calcium standards contained 5% trichloroacetic acid and 7.5 mM $LaCl_3$. Ca^{2+} absorption was linear despite the low concentrations (0.003–0.01 mM).

Na^+ fluxes, Na_i^+ and K_i^+

The techniques for measuring the bidirectional $^{22}Na^+$ fluxes, net $^{23}Na^+$ fluxes, Na_i^+ and K_i^+ have been described previously in detail [22, 23]. In brief, the Na^+ efflux was measured as the rate of appearance of tracer Na^+ in the extracellular medium after preloading the cells with $^{22}Na^+$. Na^+ influx was assessed by determining the rate of appearance of $^{22}Na^+$ in erythrocytes placed in solutions with $^{22}Na^+$. All net fluxes were calculated by sequential measurement of Na_i^+ and K_i^+ utilizing cells washed with 295 mosM $MgCl_2$, lysed in dilute Li^+ solutions and analyzed by flame photometry. The inhibitors ouabain and ethacrynic acid were used in concentrations of 0.1 and 1.0 mM, respectively. The standard flux solution, for both net and tracer studies, contained: 130 NaCl, 5 mM KCl, 10 mM glucose, 1.2 mM phosphate (as Na_2HPO_4–NaH_2PO_4, pH 7.4); 0.1 g albumin per 100 ml solution; and glycylglycine–$MgCO_3$ buffer pH 7.4 at 37 °C, 27 mM and 4.4 mM respectively.

Stereoscan electron microscopy

Packed erythrocytes were fixed for 90 min in 2% glutaraldehyde in 0.1 M cacodylate buffer (pH 7.3). Thereafter the cells were washed three times with distilled water and placed on glass coverslips. The coverslips were fastened to specimen examining stubs with silver conducting paint and Duco cement (1:1 mixture). The specimens were vacuum evaporated ($1 \cdot 10^{-5}$ Torr) and coated with light carbon (100 Å) and gold–palladium (150–200 Å) coats. These samples were examined with a Cambridge Mark III Stereoscan unit with a 20 kV beam at either a 30° or 45° angle or tilt.

RESULTS

The effects of red blood cell Ca^{2+} (Ca_i^{2+}) on Na^+ efflux are shown in Table I. Ca_i^{2+} was increased through overnight incubation of normal erythrocytes in trinitrocresol solutions with 5 mM Ca^{2+} (moderate), 10 mM Ca^{2+} (high) or zero Ca^{2+} (control). It is clear that active $^{22}Na^+$ efflux (ouabain-inhibited) decreased as Ca_i^{2+} increased. However, the ouabain-uninhibited, ethacrynic acid-inhibited Na^+ efflux [23, 24] was unaffected by Ca_i^{2+}. Na_i^+ rose and K_i^+ fell as Ca_i^{2+} was increased. In fact these latter changes of Na_i^+ and K_i^+ were minimized through the use of low Na_0^+, high K_0^+ overnight incubation media (see Methods). The separation of the data into moderate Ca_i^{2+} and high Ca_i^{2+} groups is somewhat arbitrary and Fig. 1 depicts these data for all levels of Ca_i^{2+}. Ouabain-inhibited Na^+ efflux diminished linearly as a function of log Ca_i^{2+}. Intracellular ATP was measured in several experiments in order to obtain assurance that the refrigeration in trinitrocresol solutions did not cause ATP depletion and to be certain that normal Ca_i^{2+} and high Ca_i^{2+} cells had the same ATP concentration. ATP, in the erythrocytes, was 0.85–1.0 mmole per l cells and was equal in control and high Ca_i^{2+} cells.

It seemed likely that Na^+ influx would also be affected by changes of Ca_i^{2+} since changes of K^+ permeability have been well documented. Three experiments were done in which Ca_i^{2+} was altered in the same fashion as for the efflux studies and $^{22}Na^+$ influx was assessed. Five concentrations of Ca^{2+} (0, 2.5, 5.0, 7.5 and 10 mM were provided in the loading solutions in order to obtain cells with a range of values for Ca_i^{2+}. Fig. 2 shows Na^+ influx as a function of log Ca_i^{2+}. The enhanced Na^+ influx due to elevated Ca_i^{2+} became apparent above 0.2 mM Ca_i^{2+} when these paired studies were analyzed. The enhancement of Na^+ influx after elevation of Ca_i^{2+} was significant, $P < 0.01$ when a test for trend based on ranks was used [25].

TABLE I

THE EFFECTS OF INCREASED Ca_i^{2+} ON ERYTHROCYTE Na^+ EFFLUX

Ca_i^{2+} was increased through overnight 2 °C exposure of the red blood cells to media containing 0 mM Ca^{2+} (control), 5 mM Ca^{2+} (moderate) and 10 mM Ca^{2+} (high). All overnight solutions contained 1 mM trinitrocresol to enhance Ca^{2+} entry into the cell; 10 mM Na^+, 147 mM K^+ and 2 mM Mg^{2+} (all chloride salts) were also present. The trinitrocresol was removed by six washes in a similar medium free of trinitrocresol, and three washes with isosmotic NaCl. ${}^eM_{Na}^{ouab}$ is the ouabain-inhibited Na^+ efflux and ${}^eM_{Na}^{etha}$ is the ethacrynic acid-inhibited Na^+ efflux in the presence of ouabain. Data are expressed as mean ± S.E., $n = 4$.

		Intracellular cation (mmole/l cells)			Sodium efflux (mmole/l cells/h)	
		Ca_i^{2+}	Na_i^+	K_i^+	${}^eM_{Na}^{ouabain}$	${}^eM_{Na}^{etha}$
Control	(4)	0.016±0.007	12.3±1.5	103±4	2.27±0.14	0.64±0.10
Moderate Ca_i^{2+}	(4)	0.37±0.09*	15.3±2.4	88±3**	1.29±0.18*	0.80±0.12
High Ca_i^{2+}	(4)	0.87±0.27*	18.6±4.1	76±7**	1.04±0.17*	0.90±0.13

* t test; $P < 0.01$, compared to control cells.
** t test; $P < 0.05$, compared to control cells.

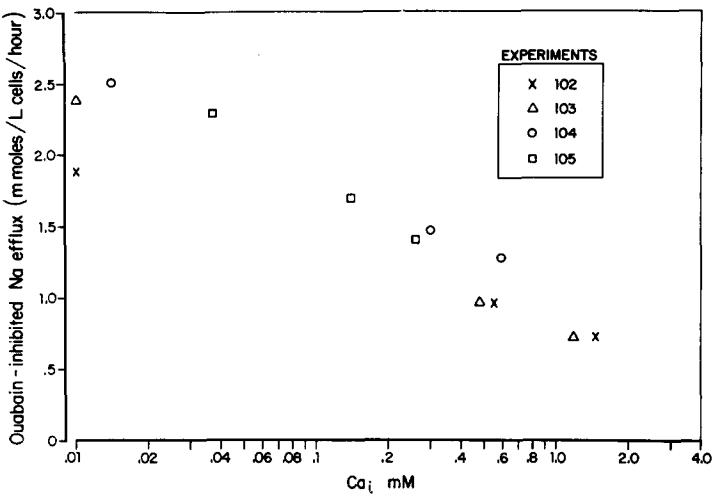

Fig. 1. The relationship of Ca_i^{2+} and ouabain-inhibited Na^+ efflux (for the experiments summarized in Table 1). Raising Ca_i^{2+} always depressed active Na^+ efflux. The values for Ca_i^{2+} were determined before the erythrocytes were loaded with ^{22}Na and the efflux measured; hence Ca_i^{2+} during the Na^+ efflux was substantially ($\pm 90\,\%$) less than the values listed. However the data in Fig. 4 show that the abnormalities of Na^+ transport persist for 3 h despite rapid reduction of Ca_i^{2+}. The composition of the flux solutions for these studies and those of Fig. 2 was identical and is described in the Methods section.

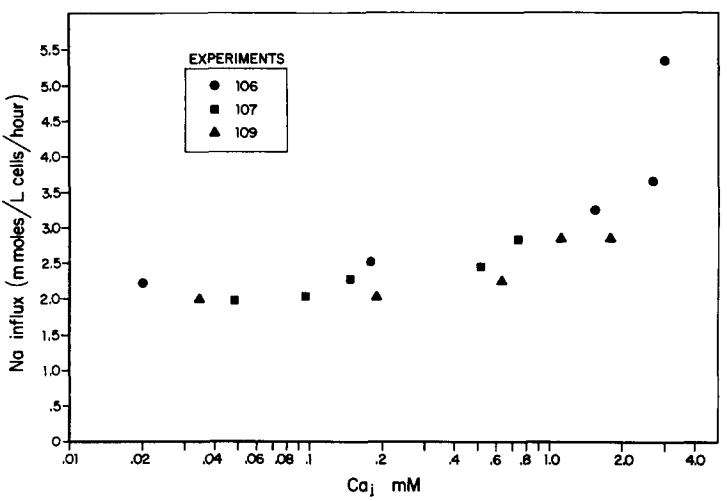

Fig. 2. Effects of Ca_i^{2+} on Na^+ influx. Ca_i^{2+} was increased using similar techniques to those in experiments in Fig. 1. The enhanced Na^+ permeability as measured by Na^+ influx was not apparent until Ca_i^{2+} exceeded 0.1–0.2 mM and was unequivocal above Ca_i^{2+} values of 0.8–1.0 mM. The trend is more obvious if the results from the single paired experiments are followed sequentially as Ca_i^{2+} was increased. $P < 0.01$ [28].

Net fluxes of Na^+ and K^+ were determined in all studies by serial measurement of Na_i^+ and K_i^+. During the 60 min efflux studies the control cells gained K_i^+ and showed no change of Na_i^+; in the cells with increased Ca_i^{2+}, Na_i^+ rose and K_i^+ fell in direct relation to the levels of Ca_i^{2+}. It should also be noted (Table I) that the zero-time values of Na_i^+ and K_i^+ showed the expected elevation and depression respectively as a function of Ca_i^{2+}. The net changes of Na_i^+ and K_i^+ during the 90 min influx experiments were very similar to those observed in the efflux studies. As Ca_i^{2+} was increased the K_i^+ losses exceeded the Na_i^+ gains and hence total intracellular electrolyte content was diminished. Fig. 3 shows the progressive fall of Na_i^+ and K_i^+ as Ca_i^{2+} increased in all studies.

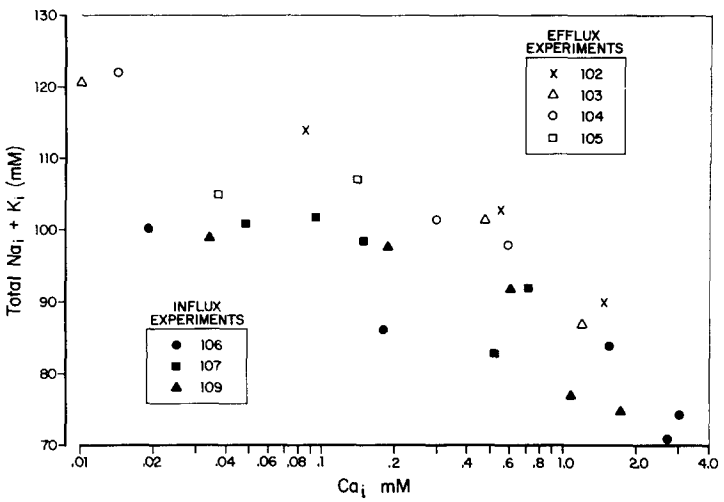

Fig. 3. The relationship between Ca_i^{2+} and total intracellular monovalent cations. The sum of Na_i^+ and K_i^+ decreased as Ca_i^{2+} increased since K_i^+ losses exceeded Na_i^+ gains. Cellular volume, as assessed by mean diameters, decreased as total intracellular Na^+ and K^+ diminished.

Two types of experiments were conducted to assess the reversibility of the Ca_i^{2+}-induced defect. These were net flux and tracer flux studies. Fig. 4 shows one of five net flux experiments which followed Ca_i^{2+}, Na_i^+ and K_i^+ over 22–24 h. The control cells were treated identically to the high Ca_i^{2+} cells except that they were not exposed to a high Ca^{2+} solution. These experiments showed: (1) Ca_i^{2+} efflux is rapid in these cells with adequate ATP concentrations and is 95% complete after 3 h (erythrocyte ATP concentration was measured in two experiments at zero time and was 0.85 and 0.40 mmole/l cells; control and high Ca_i^{2+} cells had equal concentrations of ATP); (2) the incubation solution is reasonably satisfactory since control K_i^+ and Na_i^+ were normal at 22 h; (3) after initial deterioration (away from normality) of K_i^+ and Na_i^+, there was a progressive recovery which began after Ca_i^{2+} was pumped out of the cells. Hence we concluded that the pump and leak changes (cf. Figs 1 and 2) must have been partially reversible. Over this study period Na_i^+ and K_i^+ were never observed to return to entirely normal levels. Table II shows the results of two experiments in which the ouabain-inhibited $^{22}Na^+$ efflux was measured

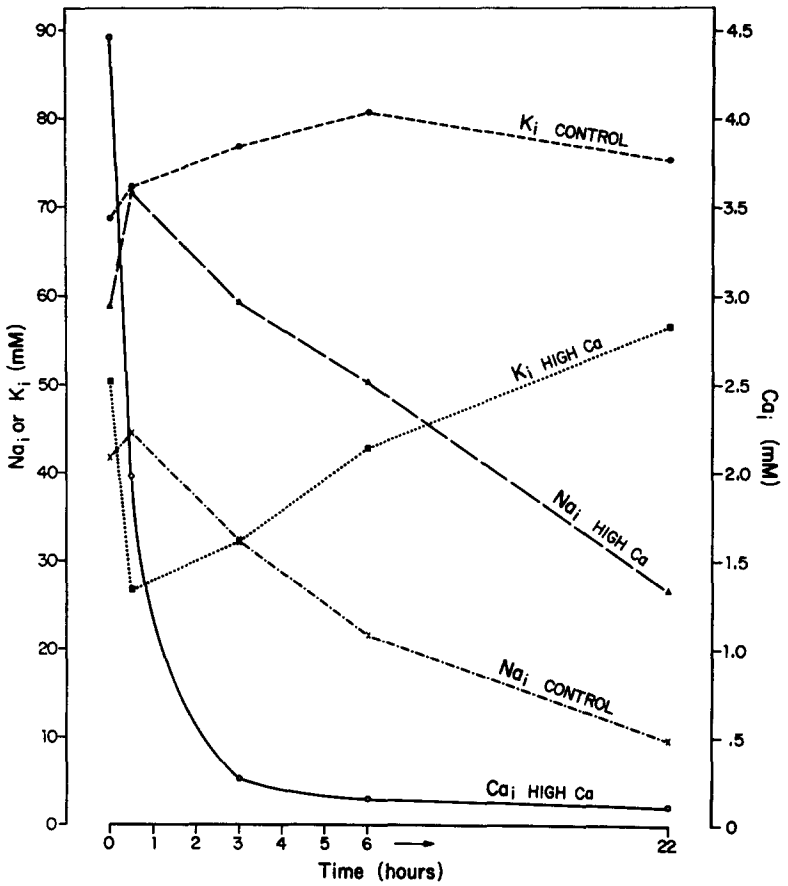

Fig. 4. The reversibility of the Ca^{2+}-induced changes of Na_i^+ and K_i^+. Control or normal-Ca_i^{2+} and high-Ca_i^{2+} erythrocytes were incubated for 22 h at 37 °C in a sterile solution containing 140 mM NaCl, 5 mM KCl, glycylglycine–$MgCO_3$ buffer, pH 7.4, 27 mM and 4.4 mM, respectively, 1.2 mM Na_2HPO_4–NaH_2PO_4 (pH 7.4), 10 mM glucose, 0.1 g albumin per 100 ml, 3 mM adenine, 10 mM inosine and 20 g/ml cephalothin (Keflin). This depicts one of five similar experiments all of which had similar results. Na_i^+ and K_i^+ were purposely altered in the control cells so that they resembled closely the high-Ca_i^{2+} cells.

before and after a 24 h incubation with control and high Ca_i^{2+} cells. If the results depicted in Fig. 4 were a consequence of improved active Na^+–K^+ transport, then increased active Na^+ efflux should be found in unidirectional tracer Na^+-efflux studies. This was the case and the data are given in Table II. The active Na^+-efflux data in Table II have been presented as rate constants rather than as mmoles of Na^+ efflux. This is important since expression of the results as mmoles of Na^+ efflux obscures the actual improvement of the pump since Na_i^+ was decreasing progressively (cf. discussion below). Once again reversibility was not complete, in that Na_i^+ and K_i^+ did not return to normal, but in each study the ouabain-inhibited Na^+–efflux ("pump") rate constant ($^e k_{Na}^{ouab}$) increased in the high Ca_i^{2+} cells after 24 h incubation despite a small fall of the same parameter in the control cells.

TABLE II

THE REVERSIBILITY OF Ca^{2+}-INDUCED CHANGES OF THE Na^+-EFFLUX PUMP

Control and experimental cells were sequentially handled as follows: (1) Refrigeration overnight in trinitrocresol solutions without and with 10 mM $CaCl_2$; (2) $^{22}Na^+$ loading; (3) $^{22}Na^+$ efflux study; (4) 24 h incubation at 37 °C in buffered sterile flux solution; (5) repeat $^{22}Na^+$ loading; (6) repeat $^{22}Na^+$ efflux study. $^{e}k_{Na}^{ouab}$ is the ouabain-inhibited Na^+-efflux rate constant.

	Intracellular cation (mmole/l cells)			Sodium efflux
	Ca_i^{2+}	Na_i^+	K_i^+	$^{e}k_{Na}^{ouab}$
Expt 117				
Control				
Zero	0.026	11.5	87	0.213
24 h	0.037	9.2	89	0.164
High Ca_i^{2+}				
Zero	1.74	24.3	54	0.065
24 h	0.085	12.8	67	0.126
Expt 124				
Control				
Zero	0.003	12.4	93.5	0.221
24 h	0.022	9.9	82.8	0.193
High Ca_i^{2+}				
Zero	0.81	19.2	80	0.114
24 h	0.05	13.2	74.2	0.163

Morphologic changes

A morphologic assessment of high-Ca_i^{2+} erythrocytes was made using scanning electron microscopy [26, 27]. Control cells were always processed similarly to high-Ca_i^{2+} cells except for the elevation of Ca_i^{2+}. Morphologic studies were conducted in parallel with the experiments shown in Table II and additional morphologic studies were done without concomitant flux data. The changes described were similar in both circumstances. The staging system for erythrocyte morphology proposed by Brecher and Bessis [26] was used: Stage 1 = slight irregularity of cellular membrane; Stage 2 = early echinocyte with spicules; Stage 3 = more spherical echinocyte or crenated cell; Stage 4 = spherocytes with few spicules. These stages merge and the classification represents a continuum of deterioration as originally stressed by Ponder [28]. Cells refrigerated in trinitrocresol without Ca^{2+} showed minor alterations of morphology as shown in Fig. 5. These changes resulted in predominately Stage 1 and occasionally stage 2 cells. These erythrocytes served as controls since they were exposed to trinitrocresol but Ca_i^{2+} remained normal. Figs 6 and 7 show the morphologic alterations of high Ca_i^{2+} cells. Fig. 6 represents a panorama, so to speak, of the Ca_i^{2+}-induced discocyte to echinocyte transformation. Whereas other experiments often showed more severe alterations, this figure was selected since all four stages of change are included. Fig. 7 is a higher power view of a Stage 3 echinocyte in a high Ca_i^{2+} cell. Many previous studies have used ATP depletion of erythrocytes as a means of creating high Ca_i^{2+} cells [3, 4, 7, 8]. Since the Ca^{2+} efflux mechanism depends upon ATP as the energy for transport. This has disadvantages since energy depletion

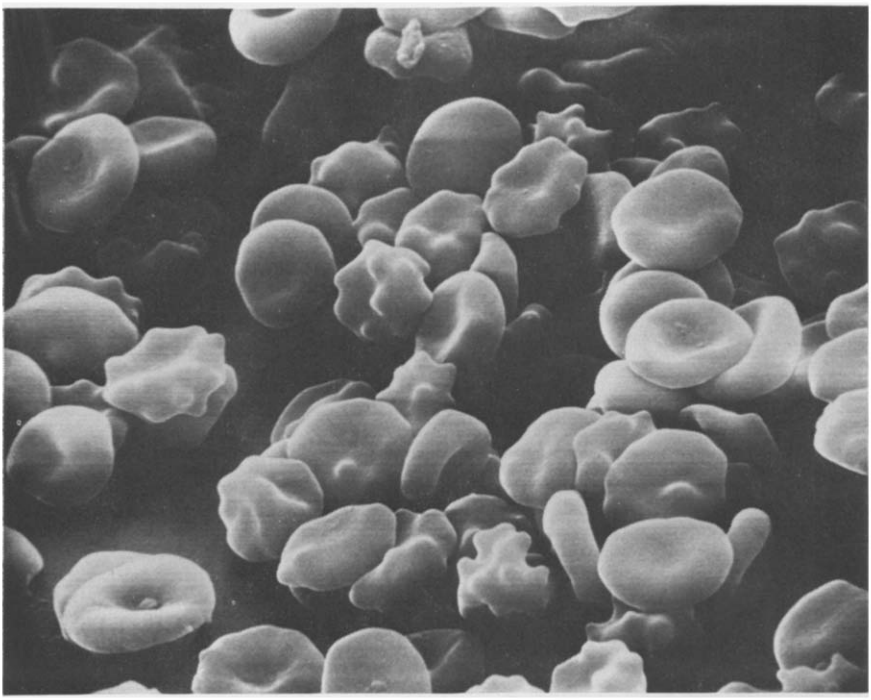

Fig. 5. Scanning electron microscopic picture of control cells after overnight exposure at 2 °C to the trinitrocresol medium (cf. Methods and Table I for composition of the refrigeration medium). Cells were either normal or showed early spicule formation (Stage 1–2). Magnification 2600×.

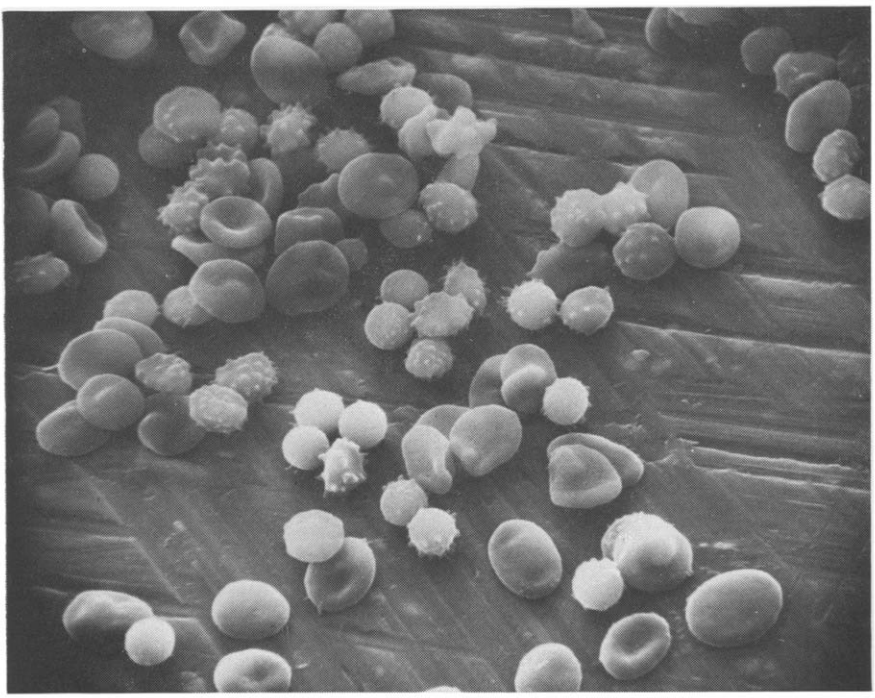

Fig. 6. High-Ca_i^{2+} erythrocytes — a typical field. High-Ca_i^{2+} erythrocytes showing all four stages of echinocytic deterioration including the final stage of microspherocytosis. Ca_i^{2+} was 0.81 mmole/l cells. Magnification 1420×.

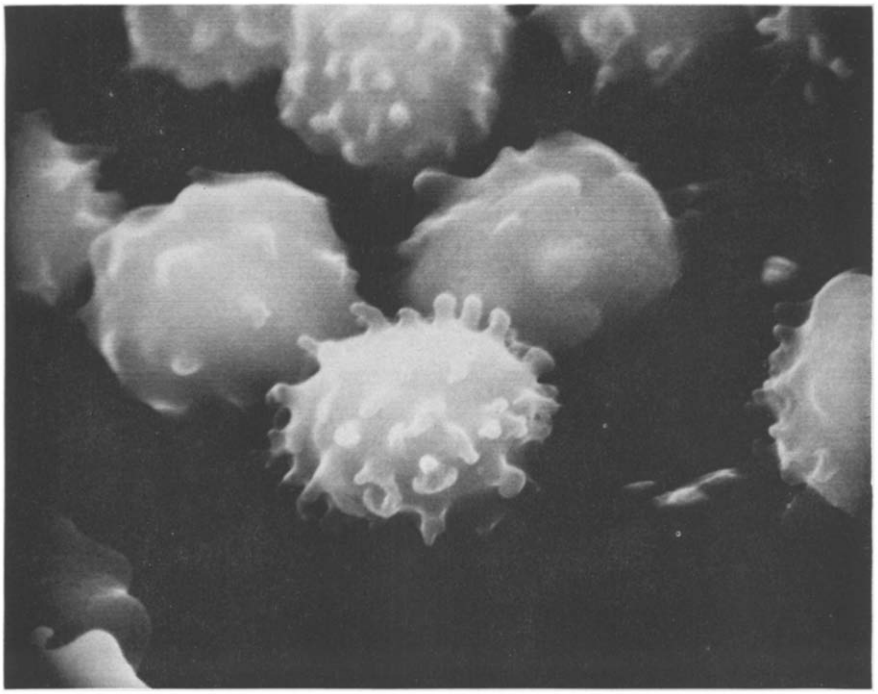

Fig. 7. High-Ca_i^{2+} erythrocytes. A Stage 3 echinocyte in the high-Ca_i^{2+} series. Magnification 7800×.

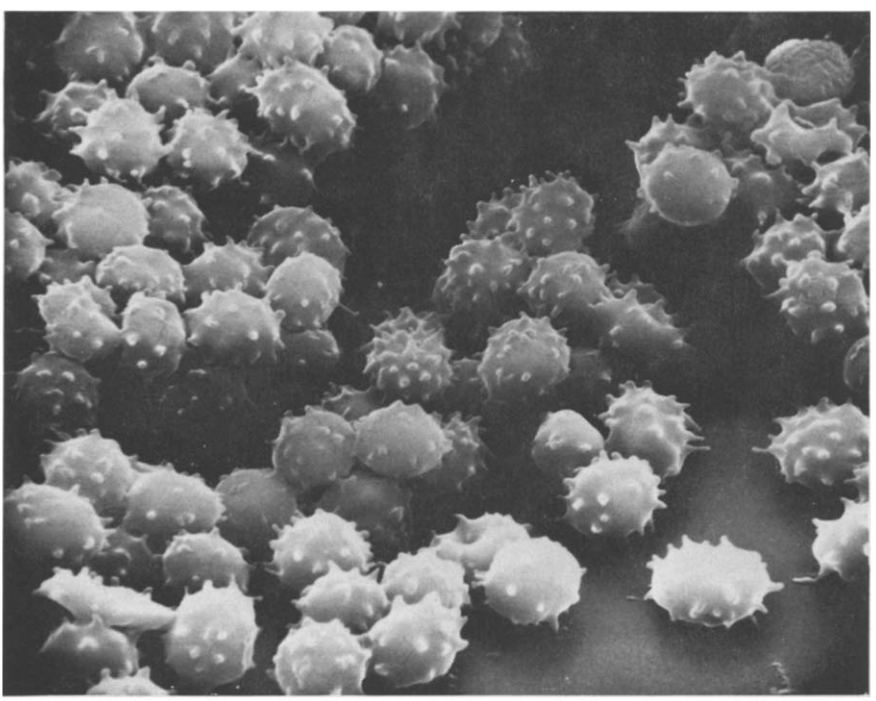

Fig. 8. ATP-depleted cells. Erythrocytes depleted of ATP by 18 h incubation at 37 °C in buffered flux solution without glucose. There was no Ca^{2+} in the solution and hence Ca_i^{2+} was not increased. Table III gives additional pertinent data. Magnification 2400×.

TABLE III

THE EFFECTS OF INTRACELLULAR Ca^{2+} AND ATP DEPLETION ON ERYTHROCYTE MORPHOLOGY

The staging was done by scanning electron microscopy using Brecher and Bessis' morphologic classification (see text for details). The number of cells examined refers to the staging; about one-third that number were measured for mean diameter. The trinitrocresol exposed cells were refrigerated for 18 h in 1 mM trinitrocresol in zero and 10 mM $CaCl_2$ solutions containing 10 mM NaCl, 120 mM KCl, and 20 % $MgCO_3$–glycylglycine buffer (v/v). The ATP-depleted cells were incubated at 37 °C for 24 h in zero and 10 mM $CaCl_2$ containing the same concentrations of Na^+, K^+ and buffer.

	Ca_i^{2+} (mm)	Morphologic staging (% of cells)						Size (diameter) Mean (μm)±S.E.
		Normal	1	2	3	4	No. of cells examined	
Trinitrocresol								
Normal Ca_i^{2+}	0.011	73	15	12	0	0	253	5.98±0.12
High Ca_i^{2+}	4.37	24	1	0	51	24	381	4.54±0.06*
ATP depletion								
Normal Ca_i^{2+}	0.012	0	0	2	98	0	179	4.64±0.07*
High Ca_i^{2+}	2.44	0	2	4	94	0	245	4.78±0.07*

* t test, $P < 0.0005$, compared to normal Ca_i^{2+} cells, trinitrocresol series.

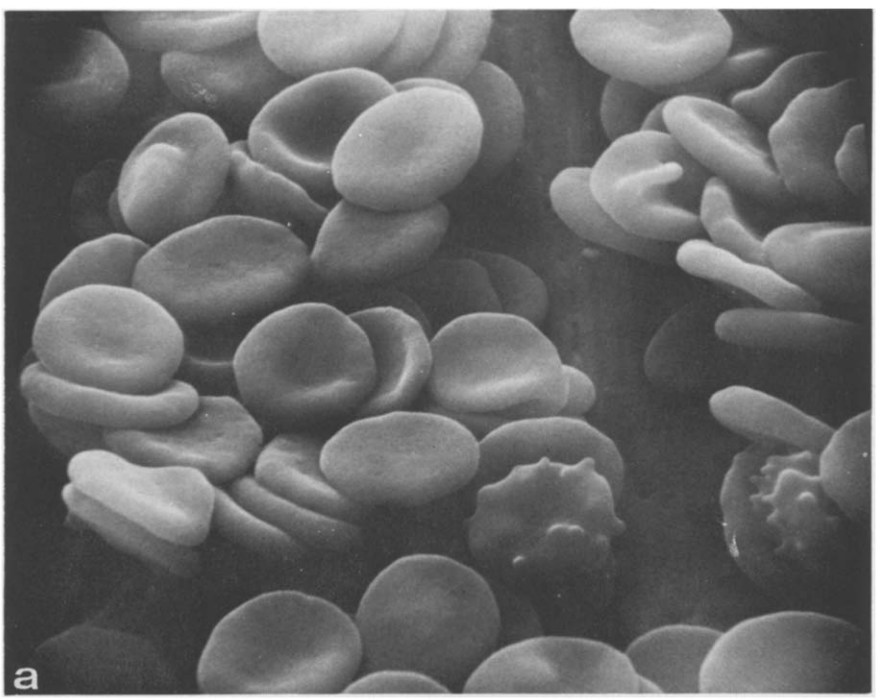

Fig. 9a. For legend see p. 109.

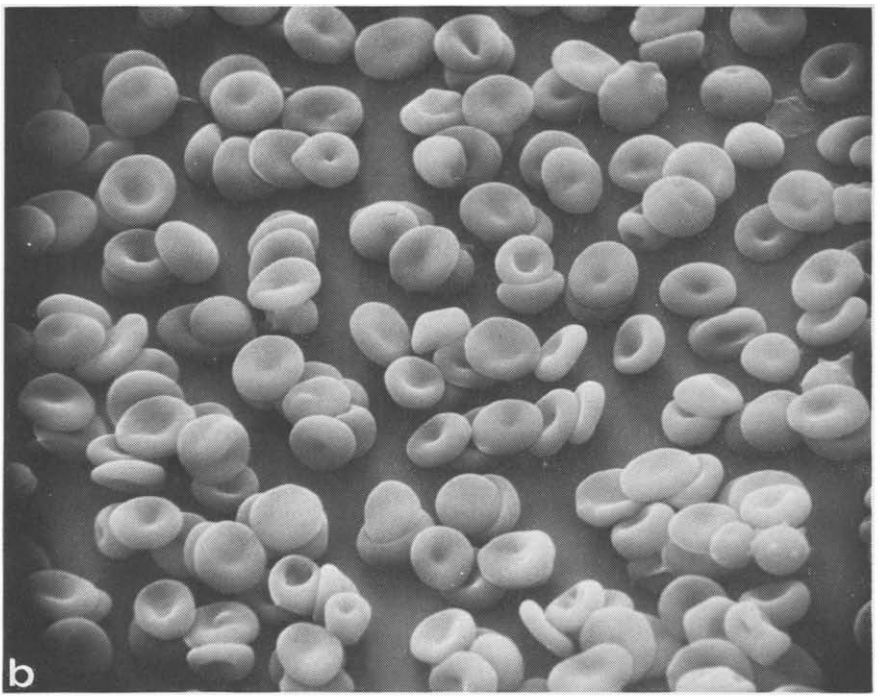
b

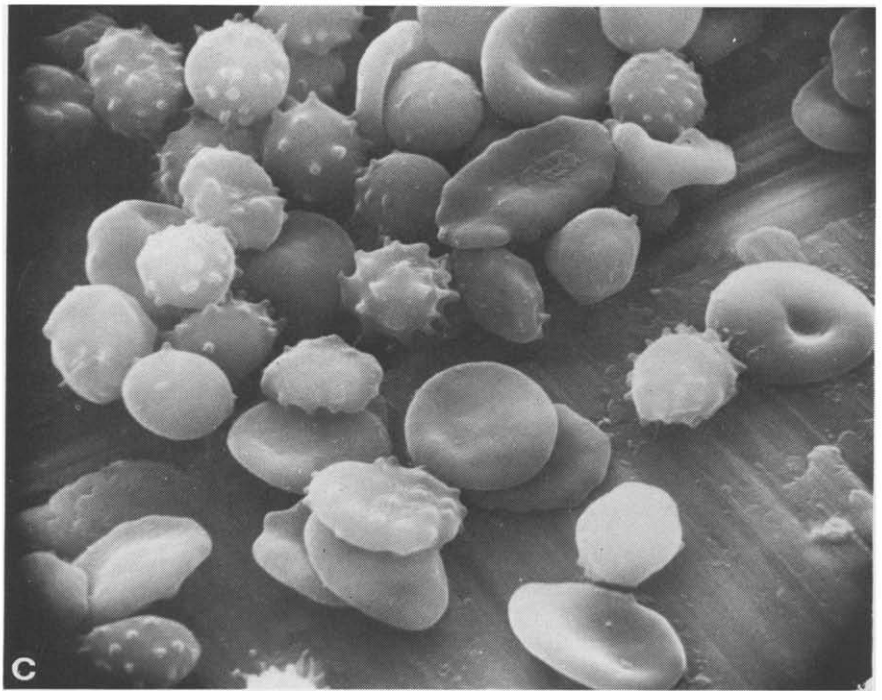
c

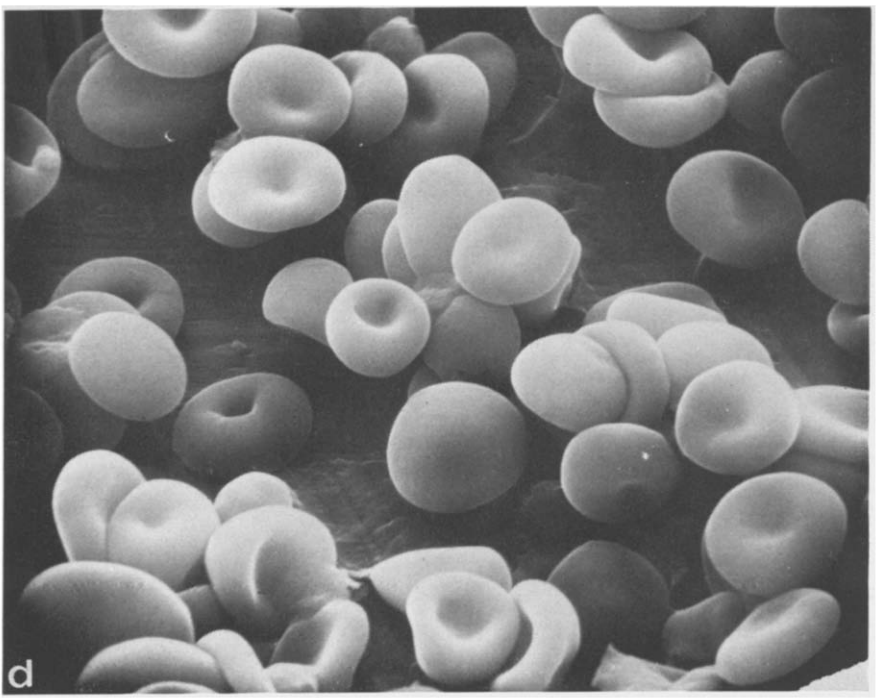

Fig. 9. Scanning photos of control and high-Ca_i^{2+} cells before and after a 24 h incubation. Figs 9(a–d) were obtained in Expt 124, Tables II and IV. (a) Normal-Ca_i^{2+} control cells after trinitrocresol exposure at 2 °C but prior to the 24 h incubation at 37 °C. Magnification 2850×. The composition of the incubation solutions is given in the legend to Fig. 4. (b) Erythrocytes, shown in (a), after 24 h incubation in trinitrocresol-free medium. Magnification 1450×. (c) High-Ca_i^{2+} erythrocytes (Expt 124) prior to incubation for assessment of the reversibility of the changes. Magnification 2860×. (d) The same series of erythrocytes shown in (c) after 24 h incubation at 37 °C. Some stomatocytes have appeared but the spiculated forms have disappeared. Magnification 2920×.

may induce separate changes. Fig. 8 shows a typical field of ATP-depleted erythrocytes (18 h without substrate) which have a normal Ca_i^{2+} since the depletion-medium was Ca^{2+}-free. Practically all cells were Stage 3 sphero-echinocytes and no cells were normal. The addition of Ca^{2+} to the ATP depletion solutions caused no further alterations of the cells even though Ca_i^{2+} was increased. These severe changes, attributable to ATP depletion alone, re-enforced our belief that trinitrocresol exposure was a preferable method of raising Ca_i^{2+}. Table III quantitaties these changes of cellular shape due to trinitrocresol exposure with and without elevation of Ca_i^{2+} and ATP depletion with and without elevation of Ca_i^{2+}.

The reversibility of the morphologic changes in the high Ca_i^{2+} erythrocytes was followed in the course of the experiments listed in Table II when net and tracer fluxes were measured before and after a 24 h incubation at 37 °C in a substrate rich medium designed to facilitate Ca^{2+} efflux and repair of the observed abnormalities of Na^+ and K^+ transport. Figs 9(a–d) are typical scanning electron micrographs from Expt 124. Figs 9(a) and 9(b) show normal Ca_i^{2+}, trinitrocresol-exposed cells at zero and 24 h, respectively. In these control cells the normal morphology was preserved and the early changes disappeared over the 24 h. Figs 9(c) and 9(d) show

TABLE IV

THE REVERSIBILITY OF MORPHOLOGIC CHANGES IN HIGH-Ca_i^{2+} ERYTHROCYTES

These studies coincided with those shown in Table II. Scanning electron microscopy was used for staging the cells. See Table II and text for experimental details. The number of cells examined refers to the quantitative staging; about one-third that number were measured for diameter.

	Morphologic stages (% of cells)						Size (diameter) Mean (μm)±S.E.
	Normal	1	2	3	4	No. of cells examined	
Expt 117							
Control							
Zero	33	10	52	5	0	120	6.84±0.10
24 h	95	4	0	0	1	81	6.38±0.15*
High Ca_i^{2+}							
Zero	50	4	4	38	4	74	5.70±0.17**
24 h	90	1	0	1	8	198	6.68±0.18***
Expt 124							
Control							
Zero	89	10	1	0	0	168	6.74±0.09
24 h	94	1	3	0	2	82	5.91±0.12**
High Ca_i^{2+}							
Zero	61	4	4	28	3	130	5.45±0.17**
24 h	85	3	2	1	9	111	5.37±0.11

* t test; mean size different from normal Ca_i^{2+}, control cells zero time, $P < 0.01$.
** t test; mean size different from normal Ca_i^{2+}, control cells zero time, $P < 0.0005$.
*** t test; mean size different from normal Ca_i^{2+}, zero time, $P < 0.005$.

high Ca_i^{2+}, trinitrocresol-exposed cells at zero and 24 h, respectively. In general the morphology improved strikingly especially with the elimination of spiculated Stage 3 forms, although there was an increase to 4–5% in Stage 4 sperocytes. Table IV shows the quantitative staging in these experiments and documents the general morphologic improvement in the high Ca_i^{2+} erythrocytes after 24 h incubation. The values, determined concomitantly, of Ca_i^{2+}, Na_i^+ and K_i^+ are given in Table II. It should also be noted that high Ca_i^{2+} erythrocytes were smaller than the normal Ca_i^{2+} controls at zero time and in Expt 117, cellular size increased after Ca_i^{2+} returned towards normal whereas in Expt 124, the mean diameter of the cells were unchanged despite substantial reduction of Ca_i^{2+}. This may be attributable to a decrease of total intracellular cations since K_i^+ did not rise. Percentage hemolysis was followed during several studies of the reversibility of the morphological changes since it was conceivable that all abnormal cells were lysed and the normal appearing cells at 24 h was an artifact of selection. Percentage hemolysis was substantially less than the percent reversibility. In one study in which 75% of the high-Ca_i^{2+} cells returned to normal appearance microscopically, only 3–5% of the cells were lost by hemolysis.

Effects of Mg^{2+} on Na^+ transport

Because of the substantial effects of Ca_i^{2+} upon the erythrocytes, we studied the consequences of decreasing and increasing intracellular Mg^{2+} (Mg_i^{2+}) on tracer Na^+ efflux. Mg_i^{2+} was altered during a 24–48 h exposure of erythrocytes to 0.1 mM

TABLE V

THE EFFECTS OF DECREASED Mg_i^{2+} ON ERYTHROCYTE SODIUM EFFLUX

The cells were incubated in glucose-free solutions for 4–24 h to deplete them of ATP. They were then exposed at 2–4 °C to 0.1 mM PCMBS, Mg^{2+}-free (low-Mg_i^{2+}) and 2 mM $MgCl_2$ (control) solutions with 10 mM Na^+ and 147 mM K^+. After 36–48 h, the cells were removed and reconstituted for 3 h at 37 °C in a medium containing 5 mM dithiothreitol, 3 mM adenine, 10 mM inosine, 10 mM glucose and concentrations of the other cations identical to the PCMBS solutions. Erythrocyte ATP concentration was 1–2 mM after this reconstitution. The cells were subsequently separated by centrifugation, washed with NaCl, loaded with $^{22}Na^+$ and efflux studied as usual. Data are expressed as mean±S.E., $n = 7$.

	Intracellular cation (mmole/l cells)			Sodium efflux (mmole/l cells per h)	
	Mg_i^{2+}	Na_i^+	K_i^+	${}^eM_{Na}^{ouab}$	${}^eM_{Na}^{etha}$
Control (7)	1.5±0.2	16.4±1.6	110±4.4	1.58±0.22	0.20±0.09
Low Mg_i^{2+} (7)	1.1±0.1*	15.7±1.2	108±3.3	1.38±0.17	0.17±0.09

* t test; $P < 0.001$ compared to control cells.

TABLE VI

THE EFFECTS OF INCREASED Mg_i^{2+} ON ERYTHROCYTE SODIUM EFFLUX

These experiments were conducted in a fashion similar to those of Table V except that the ATP depletion was omitted and the Mg^{2+} concentration of the extracellular medium for Mg^{2+} loading was 40 mM. Two different levels of $Mg^{2+}{}_i$ were achieved by varying the period of PCMBS and Mg^{2+} exposure to 16 h and 24 h. Data are expressed as mean±S.E.

	Intracellular cation (mmole/l cells)			Sodium efflux (mmole/l cells per h)	
	Mg_i^{2+}	Na_i^+	K_i^+	${}^eM_{Na}^{ouab}$	${}^eM_{Na}^{etha}$
Control (5)	2.1±0.1	9.8±1.2	109.6±1.8	1.77±0.25	0.36±0.06
High Mg_i^{2+} (4) (16 h)	6.0±0.4*	9.4±0.8	91.3±3.4	3.02±0.20**	0.46±0.11
High Mg_i^{2+} (4) (24 h)	10.1±0.5*	12.1±1.7	87.4±3.0*	2.88±0.31***	0.42±0.07

* t test; $P < 0.001$, compared to control cells.
** t test; $P < 0.01$, compared to control cells.
*** t test; $P < 0.02$, compared to control cells.

PCMBS at 2–4 °C. We found it best to deplete the cells of ATP prior to PCMBS exposure since ATP chelates Mg_i^{2+} and thereby appeared to interfere with efforts to remove Mg_i^{2+} from the cell. After the period of refrigeration, the ATP was regenerated and the sulfhydryl inhibition (PCMBS) removed through a 3 h incubation at 37 °C in simulated plasma containing adenine, inosine and dithiothreitol (cf. Methods for details). Table V summarizes these results. Despite a significant reduction of Mg_i^{2+} to 1.08±0.13 mM there was no change in ouabain-inhibited Na^+ efflux or in the ethacrynic acid-inhibited fraction of efflux between controls and low-Mg_i^{2+} cells. Mg_i^{2+} was increased in erythrocytes using techniques similar to those for decreasing Mg_i^{2+} except that the initial ATP depletion step was omitted and extracellular Mg^{2+}

was 40 mM ($MgCl_2$) during the PCMBS exposure. Two series of high-Mg_i^{2+} cells were obtained by limiting exposure to the high-Mg^{2+} medium to 16 h in one group and 24 h in another. Elevation of Mg_i^{2+} to 6.0±0.4 mM in the 16 h group and to 10.1± 0.5 mM in the 24 h group was accompanied by a 60% increase in the ouabain-inhibited Na^+ efflux as compared to the normal-Mg_i^{2+} controls (Mg_i^{2+}, 2.1±0.1 mM). Table VI summarizes these results. The high-Mg_i^{2+} cells had a lower K_i^+ than controls since $MgCl_2$ partially replaced KCl in the PCMBS medium used to raise Mg_i^{2+}.

Net Mg^{2+} efflux from erythrocytes was studied under two experimental conditions: Mg_i^{2+} was increased in normal cells using the aforementioned techniques or high Mg_i^{2+} erythrocytes were obtained from a patient with terminal renal failure. When Mg_0^{2+} exceeded Mg_i^{2+} (hence Mg^{2+} efflux was uphill) no net Mg^{2+} efflux could be demonstrated. When Mg_0^{2+} was either zero or 0.8 mM and Mg_i^{2+} was 5.0–8.7 mM (four studies), a net Mg^{2+} efflux of 0.6–2.3 mmole/l cells per 24 h was documented. Downhill Mg^{2+} efflux was similar in the cells from the uremic patient and in the "normal" high-Mg_i^{2+} cells.

DISCUSSION

Until recently there was debate over the presence of Ca^{2+} within human erythrocytes. Within the last decade, it has been established that Ca_i^{2+} is definitely present albeit at low concentrations of ±0.015 mM [29]. Furthermore it is now established that Ca_i^{2+} is low relative to plasma Ca^{2+} because of an active Ca^{2+} efflux mechanism which utilizes ATP and Ca^{2+}-stimulated ATPase [10–13]. This Ca^{2+} efflux mechanism can accomplish net Ca^{2+} transport against an electrochemical gradient and undoubtedly serves to maintain low levels of Ca_i^{2+}. In the present study we set out to evaluate the effects of increased Ca_i^{2+} on cation transport and morphology in human erythrocytes. Previous studies of this matter have led to the conclusion that Ca^{2+} affects the erythrocyte membrane only if exposed to the inner surface; changes of extracellular Ca^{2+} are without effect [14, 15]. A variety of methods have been used to raise Ca_i^{2+} and assess membrane function. The most popular techniques have used resealed erythrocyte ghosts or ATP-depleted whole cells [2, 3, 8]. The ghost method has the intrinsic disadvantage of a more permeable or leaky membrane as a residual of the preparation of the ghost membrane. The ATP-depleted erythrocytes lack a Ca^{2+} efflux mechanism and hence they accumulate Ca_i^{2+} in a high Ca^{2+} medium. However, the absence of ATP prohibits study of the effects of Ca_i^{2+} on active Na^+ efflux and also ATP-poor cell have intrinsic morphologic and physiologic abnormalities. These changes limit an assessment of the singular impact of Ca_i^{2+}. We therefore turned to trinitrocresol as an agent which reversibly alters membrane cation and anion permeability. Partial proof of the reversible nature of the trinitrocresol effects can be found in Table I and Fig. 2. The values for active Na^+ efflux and passive Na^+ influx in the normal Ca_i^{2+} cells approximates closely the normal values in this laboratory. Our results confirm the absolute importance to the erythrocyte of close control of the level of Ca_i^{2+}. The active (ouabain-inhibited) Na^+ efflux was inhibited at levels of Ca_i^{2+} which did not enhance Na^+ influx and as Ca_i^{2+} was further increased Na^+ efflux decreased progressively (cf. Fig. 1). These changes of $^{22}Na^+$ tracer flux reflected net changes since Na_i^+ rose in high Ca_i^{2+} cells. Our

results extend Hoffman's [2] observations made with erythrocyte ghosts resealed in Ca^{2+} media (Ca_i^{2+} not measured). When human erythrocyte ghosts were resealed in an ATP-rich, 1–3 mM Ca_o^{2+} and 0–3 mM Mg_o^{2+} solution, the rate constant for strophanthidin-sensitive Na^+ efflux decreased. Presumably this inhibition of the Na^+ pump is the result of inhibition of Na^+-and K^+-stimulated ATPase. Many investigators have reported that Ca^{2+} (intracellular level) inhibits the Na^+- and K^+-stimulated ATPase in many tissues including erythrocytes [30–32]. The mode of inhibition is uncertain but it may depend upon formation of a Ca^{2+}–ATP complex which competes with Mg^{2+}–ATP in the ATPase reaction [32]. It should be noted that despite substantial decrements of the ouabain-inhibited Na^+ efflux, there was no change or a slight increment in the ethacrynic acid-inhibited, ouabain-uninhibited Na^+ efflux. This contrasts with the situation described in uremia in which high-Na_i^+ human erythrocytes have depressed efflux rate constants for both components of efflux [33].

Elevations of Ca_i^{2+} not only reduced active Na^+ efflux but the passive downhill entry of Na^+ into the cells was also enhanced. When Ca_i^{2+} exceeded ± 0.2 mM Na^+ influx increased thereby contributing to accumulation of Na^+ in a cell unable to respond by increasing active Na^+ efflux. This combination of enhanced Na^+ permeability and depressed Na^+ efflux resembles the cellular effect of experimental malaria on erythrocytes. However, Ca_i^{2+} was not increased in erythrocytes obtained from monkeys with malaria [22]. Romero and Whittam [7] also observed enhancement of Na^+ influx in high-Ca_i^{2+} erythrocytes which were metabolically depleted. Our results show that changes of Ca_i^{2+}, without metabolic depletion, will induce substantial alterations to Na_i^+. These data contradict the conclusions of Hoffman [3] and Blum and Hoffman (see refs 14, 15) that Ca_i^{2+} affects only K^+ and not Na^+ permeability. Gardos has emphasized that Ca_i^{2+} controls K^+ permeability in erythrocytes and that the striking increase of K^+ leak in cells exposed to NaF or iodoacetate depends upon Ca^{2+} entry into the cell [1]. These changes of K^+ permeability after elevation of Ca_i^{2+} have been documented extensively. Rummel et al. [35] have also reported that high Ca_i^{2+} cells have decreased ouabain-inhibited K^+ influx. Although tracer K^+ experiments were not conducted along with the Na^+ studies of the present report, the net changes of K_i^+ suggested a reciprocal fall of active K^+ influx (since active Na^+ efflux and K^+ influx are linked) and a rise of passive K^+ efflux as Ca_i^{2+} increased. It appeared that K^+ losses exceeded Na^+ gains in the cells and total cellular cation diminished (Fig. 3). Our studies also showed a slower return to normal of K_i^+ as compared to Na_i^+ after Ca^{2+} was eliminated from the cell. This might have been predicted from previous studies which showed Ca_i^{2+} primarily affecting K^+ permeability.

Human erythrocytes, like other cells, respond to injury in a limited number of ways and in a generally predictable fashion. Years ago, Ponder [28] emphasized that disc to sphere transformation (after exposure to lysins) was accompanied by a loss of cell surface area and by intermediate stages of crenated discs and crenated spheres. Recent use of stereoscan electron microscopy has permitted more detailed investigation of these morphologic stages and has introduced the terminology of discocyte and echinocyte [26, 27]. We have used the staging proposed by Brecher and Bessis in order to quantitate the changes [26]. Our results show that increased Ca_i^{2+} results in morphologic deterioration of the cell to echinocytic and spherocytic forms. Others [8, 36] have reported similar findings using phase contrast microscopy and high-Ca_i^{2+},

energy-depleted cells. These changes are not specific for Ca_i^{2+}-induced membrane damage since many forms of cellular injury including energy-depletion alone cause a similar sequence of events. As can be seen in Figs 6 and 9, all cells are not abnormal. It is unknown whether these "normal" cells have a high Ca_i^{2+} or whether high Ca_i^{2+} affects differently cells of different ages.

Weed and co-workers [8] have suggested that the interactions of Ca^{2+}, ATP and the erythrocyte membrane are critical determinants of cellular deformability, filterability and viscosity. They hypothesize that the ATP-depleted, high-Ca_i^{2+} cell undergoes sol to gel protein transformation in the membrane. Their data suggest that Ca_i^{2+} is the more important factor and that ligands such as EDTA, which cannot provide energy for Ca^{2+} efflux, form protective chelates with Ca_i^{2+} if incorporated into depleted ghosts [8]. Our experiments extend these observations in several ways. Fig. 8 shows the severe crenation in ATP-depleted cells with normal Ca_i^{2+}. It is clear that energy depletion can induce morphologic deterioration independent of accumulation of Ca_i^{2+} [37]. On the other hand our work with the trinitrocresol-exposed, high Ca_i^{2+}, normal ATP cells (Figs 5–7, 9) confirms the detrimental impact of Ca^{2+} on the inner surface of the cell membrane apart from the consequences of ATP depletion. Intracellular energy stores, in the form of ATP, may exert control over membrane function and cell shape in at least several ways: (1) control of the active mechanism for Na^+ efflux and K^+ influx; (2) control of Ca_i^{2+} through modulation of the Ca^{2+} efflux pump or by forming Ca^{2+}–ATP chelates; (3) direct effects on the membrane apart from control of Ca_i^{2+}. It is not known whether the different actions are summational but it should be noted that the morphologic alterations induced by ATP depletion were not exaggerated when Ca_i^{2+} was also elevated (Table III). On the other hand Weed and co-workers, using more quantitative parameters of viscosity and membrane deformability saw separate and additive effects of ATP depletion and elevation of Ca_i^{2+}, although the level of Ca_i^{2+} seemed the predominant determinant [8].

The reversibility which we observed in both physiologic (transport) and morphologic parameters suggests that much of the Ca_i^{2+}-membrane interaction is dynamic and reparable. Weed et al. reported significant reversal of the changes of viscosity and membrane deformability when high Ca_i^{2+}, ATP-depleted cells were incubated for 2 h with 30 mM adenosine [8]. Romero and Whittam showed partial reversibility of the transport defects in that K_i^+ stopped decreasing or increased slightly when adenine and inosine were added to energy-depleted Ca^{2+}-rich cells [7]. The data in Table II and Fig. 4 show conclusively that the alterations of Na^+–K^+ transport can be reversed if the high-Ca_i^{2+} cells are provided the opportunity to pump the Ca^{2+} out of the cells and thereby return the Na^+–K^+ pump (and presumably Na^+–K^+ permeability) towards normal. The improvement in the Na^+ efflux rate constants (Table II) is all the more significant if one considers that control rate constants fell after the 24 h incubation. It could be argued that the results shown in Table II do not conclusively explain the decrement of Na_i^+ shown in Fig. 4. There are three reasons why we believe the decrement of Na_i^+ is mainly due to increased Na^+ efflux: (1) the major defect in high Ca_i^{2+} cells is decreased Na^+ efflux rather than increased Na^+ permeability; hence reversal of the defect must involve the pump. (2) If improved, active Na^+ efflux does not account for the return of Na_i^+ towards normal, then leak-influx of Na^+ must fall to 50% below normal to explain the net loss of Na^+ from the cells. Clearly the Na^+ efflux must have transiently exceeded Na^+ influx until Na_i^+

decreased to 10–13 mM. (3) Active Na^+ efflux decreases when Na_i^+ is reduced in normal cells. Since total active Na^+ efflux (mmoles/l cells per h) remained stable despite decreasing Na_i^+ when high-Ca_i^{2+} cells were incubated for 22–24 h, and since efflux rate constants increased significantly, we conclude that the active Na^+ efflux mechanism improved. The reversibility of most of the morphologic changes, observed with scanning electron microscopy, was impressive and unequivocal (Fig. 9). However, the Stage 4 cells, microspherocytes, appeared to be irreversibly altered.

The role of Mg_i^{2+} in human erythrocytes has not been investigated extensively [16]. Normal Mg_i^{2+} is about 2.0 mmol/l cells. Mg^{2+} depletion lowers Mg_i^{2+} and certain situations such as chronic renal failure increase Mg_i^{2+}. Mg^{2+} transport across the erythrocyte membrane occurs slowly and no evidence has been adduced in support of any active Mg^{2+} transport in erythrocytes. Just as with Ca_i^{2+} there is little information regarding the distribution of Mg_i^{2+} within the cell or the percent of ionized or bound fractions [16]. Others have shown that $Mg^2{}_i^+$ helps reseal ghost membranes, restore normal permeability after incubations with lactose [38] and antagonize the detrimental actions of Ca_i^{2+} in resealed ghosts [8]. Our present results show that moderate reductions of Mg_i^{2+} do not influence Na^+ efflux whereas elevations of Mg_i^{2+} stimulate active Na^+ efflux. These in vitro results with low-Mg_i^{2+} cells agree with in vivo results in Mg^{2+}-depleted monkeys in which reductions of Mg_i^{2+} were not accompanied by changes of Na_i^+ and K_i^+ [39]. The stimulation of ouabain-inhibited Na^+ efflux when Mg_i^{2+} was raised from 2.1 to 6–10 mM was unexpected. The explanation for this observation may be that high-Mg_i^{2+} cells contained increased levels of Mg^{2+}. Since much of the normal total magnesium may not be ionized the Na^+–K^+ ATPase probably operates below maximal efficiency. Dunham and Glynn [31] found that 2–3 mM Mg^{2+} maximally stimulated erythrocyte ghost Na^+–K^+ ATPase. The increased Na^+ efflux (Table VI) after elevations of Mg_i^{2+} may have resulted from ATPase stimulation. The stimulatory effects of Mg_i^{2+} on Na^+ efflux may explain the variable incidence of the reported defect of the Na^+–K^+ pump in uremia [33]. Since erythrocyte Mg^{2+} is invariably elevated in uremia [40] the Na^+ efflux in uremic erythrocytes is influenced by stimulatory and depressant factors. No evidence of a Mg^{2+} pump was found under the conditions studied although Mg^{2+} slowly left the high-Mg_i^{2+} cells when Mg_o^{2+} was low.

ACKNOWLEDGEMENTS

I acknowledge gratefully the excellent secretarial assistance of Mrs Jennifer Pastore and the statistical advice of Dr Kathleen Lamborn. This work was supported by Research Grant AM 14264 from the National Institutes of Health, U.S.P.H.S., and by a grant from the Markle Foundation.

REFERENCES

1 Gardos, G. (1959) Acta Physiol. Acad. Sci. Hung. 15, 121
2 Hoffman, J. F. (1962) Circulation 26, 1201
3 Hoffman, J. F. (1966) Am. J. Med. 41, 666
4 Kregenow, F. M. and Hoffman, J. F. (1972) J. Gen. Physiol. 60, 406
5 Palek, J., Curby, W. and Lionetti, F. (1971) Am. J. Physiol. 220, 19

6 Passow, H. (1963) Cell Interface Reactions, Vol. 1, pp. 57–107, H. D. Brown, New York Scholars Library
7 Romero, P. and Whittam, R. (1971) J. Physiol. 214, 481
8 Weed, R., LaCelle, P. and Merrill, E. (1969) J. Clin. Invest. 48, 795
9 Whittam, R. and Wheeler, K. P. (1970) Annu. Rev. Physiol. 32, 21
10 Lee, K. and Shin, B. (1969) J. Gen. Physiol. 54, 713
11 Olson, E. and Cazort, R. (1969) J. Gen. Physiol. 53, 311
12 Schatzmann, H. (1966) Experientia 22, 364
13 Schatzmann, H. and Vincenzi, F. (1969) J. Physiol. 201, 369
14 Blum, R. and Hoffman, J. (1972) Biochem. Biophys. Res. Commun. 46, 1146
15 Garrahan, P. J. and Glynn, I. M. (1967) J. Physiol. 192, 159
16 Walser, M. (1967) Ergeb. Physiol. Biol. Chem. Exp. Pharmakol. 59, 185
17 Gunn, R. B. and Tosteson, D. C. (1971) J. Gen. Physiol. 57, 593
18 Garrahan, P. J. and Rega, A. F. (1967) J. Physiol. 193, 459
19 Cleland, W. W. (1964) Biochem. J. 3, 480
20 Bartlett, G. R. and Bucolo, G. (1968) Biochim. Biophys. Acta 156, 240
21 Adams, H. (1965) Methods of Enzymatic Analysis (Bergmayer, H., ed.), 1st edn, p. 539, New York
22 Dunn, M. J. (1969) J. Clin. Invest. 48, 674
23 Dunn, M. J. (1970) J. Clin. Invest. 49, 1804
24 Dunn, M. J. (1973) J. Clin. Invest. 52, 658
25 Page, E. B. (1963) J. Am. Stat. Assoc. 58, 216
26 Brecher, G. and Bessis, M. (1972) Blood 40, 333
27 Lessin, L. S., Jensen, W. N. and Klug, P. (1972) Arch. Intern. Med. 129, 306
28 Ponder, E. (1948) Hemolysis and Related Phenomena, Vol. 1, pp. 26–36, Grune and Stratton, New York
29 Harrison, D. G. and Long, C. (1968) J. Physiol. 199, 367
30 Davis, P. W. and Vincenzi, F. F. (1971) Life Sci. 10, 401
31 Dunham, E. and Glynn, I. (1961) J. Physiol. 156, 274
32 Epstein, F. and Whittam, R. (1966) Biochem. J. 99, 232
33 Welt, L. G. (1969) Nephron, 6, 406
34 Blum, R. and Hoffman, J. (1971) J. Memb. Biol. 6, 315
35 Rummel, W., Seifen, E. and Baldauf, J. (1963) Biochem. Pharmacol. 12, 557
36 Szasz, I., Teitel, P. and Gardos, G. (1970) Acta Biochim. Biophys. Acad. Sci. Hung. 5, 409
37 Nakas, M., Nakas, T. and Yamazoe, S. (1960) Nature 187, 945
38 Bolingbroke, V. and Maizels, M. (1959) J. Physiol. 149, 563
39 Dunn, M. J. (1971) Clin. Sci. 41, 333
40 Contiguglia, S. R., Alfrey, A. C., Miller, N. and Butkus, D. (1972) Lancet i, 1300